Received: 29 January 2020 | Revised: 3 July 2020 | Accepted: 3 July 2020

DOI: 10.1111/ejn.14903

SPEICAL ISSUE ARTICLE

System Neuroscience

EJN European Journal of Neuroscience FENS WILEY

Weakly correlated activity of pallidal neurons in behaving monkeys

Woranan Wongmassang[1,2] | **Taku Hasegawa**[1] | **Satomi Chiken**[1,2] | **Atsushi Nambu**[1,2]

[1]Division of System Neurophysiology, National Institute for Physiological Sciences, Okazaki, Japan

[2]Department of Physiological Sciences, SOKENDAI (Graduate University for Advanced Studies), Okazaki, Japan

Correspondence
Atsushi Nambu and Satomi Chiken, Division of System Neurophysiology, National Institute for Physiological Sciences, Okazaki, Japan.
Email: nambu@nips.ac.jp and chiken@nips.ac.jp

FUNDING INFORMATION
MEXT KAKENHI "Non-linear Neuro-oscillology", 15H05873. JSPS KAKENHI, 19KK0193, 18K15340, 16K07014, 26250009. JST CREST, JPMJCR1853. AMED, JP19dm0307005.

Abstract

The basal ganglia play a crucial role in the control of voluntary movements. Neurons in both the external and internal segments of the globus pallidus, the connecting and output nuclei of the basal ganglia, respectively, change their firing rates in relation to movements. Firing rate changes of movement-related neurons seem to convey signals for motor control. On the other hand, coincident spikes among neurons, that is, correlated activity, may also contribute to motor control. To address this issue, we first identified multiple pallidal neurons receiving inputs from the forelimb regions of the primary motor cortex and supplementary motor area, recorded neuronal activity of these neurons simultaneously, and analyzed their spike correlations while monkeys performed a hand-reaching task. Most (79%) pallidal neurons exhibited task-related firing rate changes, whereas only a small fraction (20%) showed significant but small and short correlated activity during the task performance. These results suggest that motor control signals are conveyed primarily by firing rate changes in the external and internal segments of the globus pallidus and that the contribution of correlated activity may play only a minor role in the healthy state.

KEYWORDS

Basal ganglia, cross-correlation, globus pallidus, motor control, multichannel recording

1 | INTRODUCTION

The globus pallidus, a nucleus of the basal ganglia, is divided by the medial medullary lamina into the external (GPe) and internal (GPi) segments. The GPe and GPi are essential for controlling voluntary movements and posture (Wichmann & DeLong, 1996; Hauber, 1998). According to the basic circuits of the basal ganglia, the GPi and substantia nigra pars reticulata (SNr) are considered the output stations of the basal ganglia that presumably control voluntary

Abbreviations: GPe, external segment of the globus pallidus; GPi, internal segment of the globus pallidus; LED, light-emitting diode; M1, primary motor cortex; PEEK, polyether ether ketone; PETH, peri-event time histogram; PSTH, peri-stimulus time histogram; SD, standard deviation; SMA, supplementary motor area; SNr, substantia nigra pars reticulata; STN, subthalamic nucleus.

Edited by: Yoland Smith

movements (Alexander & Crutcher, 1990; Nambu et al., 2000, 2002b). They receive inputs from the striatum and subthalamic nucleus (STN), the input stations of the basal ganglia, and project to the thalamocortical and brainstem motor systems. On the other hand, the GPe is considered a connecting nucleus that controls the activity of the entire basal ganglia. The GPe receives inputs from the striatum and STN and affects GPi/SNr activity through the GPe-STN-GPi/SNr and GPe-GPi/SNr projections, with some GPe neurons projecting back to the striatum (Glajch et al., 2016; Hegeman et al., 2016).

Considering their positions in the basal ganglia circuit, analysis of the activity of GPe/GPi neurons during voluntary movements is very important to understand the functions of the basal ganglia. In monkeys, GPe/GPi neurons have shown firing rate changes that are closely related to active forelimb movements (DeLong, 1971; Hamada et al., 1990; Nambu et al., 1990; Mushiake & Strick, 1995; Turner & Anderson, 1997), but how they encode motor control remains a topic of debate. In other brain areas, correlated activity has been proposed to convey neuronal information in addition to firing rate changes (Vaadia et al., 1995; Alonso et al., 1996; Kohn, 2005; Bruno, 2006; de la Rocha et al., 2007). These neurons utilize coincident spikes to enhance the efficacy of information transmission. In monkey models of Parkinson's disease, correlated oscillatory activity was reported in GPe/GPi neurons, and its significance was discussed in the context of parkinsonian pathophysiology (Nini et al., 1995; Bergman et al., 1998; Raz et al., 2000). In healthy monkeys, on the other hand, these studies showed no such correlations at rest (Nini et al., 1995; Raz et al., 2000; Bar-Gad et al., 2003). The same group also reported that SNr neurons do not show any correlations in healthy monkeys at rest or during performance of a probabilistic delayed visuomotor response task (Nevet et al., 2004, 2007). However, correlated activity during movements has not been examined in the GPe/GPi, which are largely occupied by somatomotor areas. To address the question of whether correlated activity conveys neuronal information related to movements in the healthy state, here we identified GPe/GPi neurons receiving inputs from the forelimb regions of the primary motor cortex (M1) and supplementary motor area (SMA), simultaneously recorded the activity of multiple neurons in these areas during a hand-reaching task, and then analyzed firing rate changes and cross-correlations of neuronal pairs.

Our results revealed that the majority of GPe/GPi neurons receiving inputs from the forelimb regions of the M1 and/or SMA showed firing rate increases or decreases during reaching movements, but only a small fraction exhibited correlations during the task performance. These results suggest that motor control signals in the GPe/GPi are conveyed primarily by firing rate changes, but not by correlated activity.

2 | MATERIALS AND METHODS

2.1 | Animals

Two adult female Japanese monkeys (*Macaca fuscata*; *Monkey H*, 6 years old, 5 kg; *Monkey L*, 8 years old, 6 kg) were used in the present study. The research protocol was approved by the Institutional Animal Care and Use Committee of the National Institutes of Natural Sciences, and the study was conducted according to the guidelines of the National Institutes of Health *Guide for the Care and Use of Laboratory Animals*. Throughout the study, the body weight, activities of daily living and food intake of the monkeys were routinely monitored. The monkeys' access to water was regulated to increase their motivation to perform the task. Their body weight was kept at ≥90% of the body weight before starting the experiment.

2.2 | Hand-reaching task

Prior to the experiments, each monkey was trained to sit quietly in a monkey chair and perform a hand-reaching task (Figure 1a,b). An infrared optical imaging touch panel (ARTS-015; O'HARA) was placed in front of the monkey at a distance of 20 cm, and two light-emitting diodes (LEDs) were arranged horizontally separated by 16 cm behind the transparent touch panel. Each trial was initiated after the monkey placed its hand onto the home position for at least 300 ms (Home position). The left or right LED was randomly selected and lit (LED On). In response to the lighting of the LED, the monkey was required to release its hand from the home position (Hand Release) and to reach out to the target area indicated by the LED (Touch). The timings of Hand Release and Touch were detected by infrared photoelectric sensors (PS-46, PS-52C and FU-A100; Keyence), and the position of Touch was detected by the touch panel. If the monkey touched the target area (3 × 3 cm square centered at the LED) within 6,000 ms after LED On and held the position for at least 40 ms, the trial was considered successful, the LED was turned off and a small amount of water was dispensed as a reward (Reward) with a delay of 200 ms. The LED on the same side as the reaching hand was defined as the ipsilateral target LED (Ipsi-LED), whereas the opposite side was defined as the contralateral target LED (Contra-LED).

Minimum requirement time for placing their hands onto the home position was short (300 ms); however, monkeys did not seem to predict LED On, because (a) monkeys had to choose either the left or right target based on the target LED; (b) in most cases, monkeys returned their hands to the home position within the intertrial intervals, and thus, waiting time on the home position was variable; (c) reaction time (between LED On and Hand Release) was not too short, and both

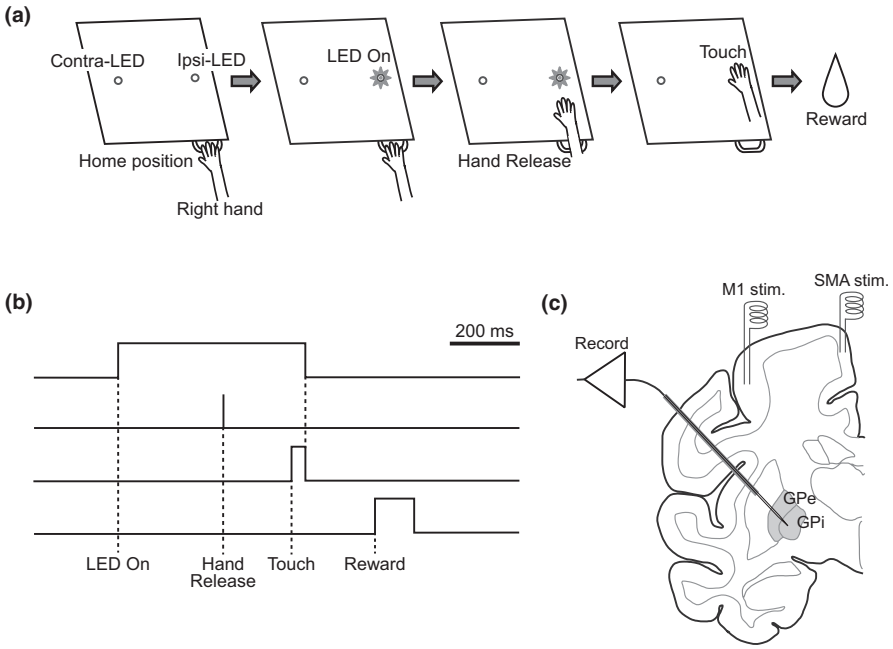

FIGURE 1 Task and experimental setup. (a, b) The hand-reaching task. Each trial was initiated when the monkey placed its hand on the home position for 300 ms (Home position). Then, a green LED was lit randomly on the left or right side of the touch screen (LED On). The LED target on the contralateral side of the reaching hand was defined as contralateral LED (Contra-LED), whereas that on the ipsilateral side was defined as ipsilateral LED (Ipsi-LED). The monkey was required to release its hand from the home position (Hand Release) and continue touching the target indicated by the LED for at least 40 ms (Touch). If the monkey touched the target within 6,000 ms after LED On, the LED was turned off, and the monkey was rewarded with water (Reward) 200 ms after Touch. (c) Schematic representation of the experimental setup for recording neuronal activity in the external (GPe) and internal (GPi) segments of the globus pallidus. Two pairs and one pair of bipolar stimulating electrodes were implanted chronically in the forelimb regions of the primary motor cortex (M1) and supplementary motor area (SMA), respectively. A multichannel recording electrode was inserted obliquely (40° from vertical) through a guide tube into the GPe or GPi for extracellular recording during the task performance

reaction time and movement time (between Hand Release and Touch) were highly variable: reaction time, 304 ± 35 and 324 ± 32 ms (Contra- and Ipsi-LED of *Monkey H*), 285 ± 27 and 287 ± 29 ms (Contra- and Ipsi-LED of *Monkey L*); movement time, 126 ± 29 and 130 ± 32 ms (Contra- and Ipsi-LED of *Monkey H*), 202 ± 50 and 183 ± 27 ms (Contra- and Ipsi-LED of *Monkey L*) (see also Figure 2b,c,e,f); and (d) no ramping activity of the GPe and GPi neurons was seen before LED On, which was a sign of predictable events (Nambu et al., 1990). Monkeys were trained daily for 1 month to achieve a success rate of more than 80%. Then, they underwent a surgical operation.

2.3 | Surgical procedures

Each monkey underwent a surgical operation to allow its head to be fixed painlessly in a stereotaxic frame attached to a monkey chair. After anesthesia with ketamine hydrochloride (5–8 mg/kg body weight, i.m.) and xylazine hydrochloride (0.5–1 mg/kg, i.m.), propofol was continuously injected intravenously during surgery using a target-controlled infusion pump (TE-371; Terumo; 6–9 μg/ml target blood concentration) with fentanyl administration (2–5 μg/kg, i.m.). The skull was widely exposed, and small screws made of polyether ether ketone (PEEK) were attached to the skull as anchors. The exposed skull and screws were completely covered with bone adhesive resin (Super-Bond C&B; Sun Medical) and transparent acrylic resin (Unifast II; GC), and then two pipes made of PEEK for head fixation were mounted and fixed on the monkey's head. All surgical procedures were performed under aseptic conditions, and the arterial oxygen saturation level and heart rate were continuously monitored during surgery. An antibiotic and analgesic (ketoprofen) were injected (i.m.) after surgery.

2.4 | Implantation of stimulating electrodes in the motor cortices

A few days after the head-fixation surgery, each monkey was positioned in a stereotaxic apparatus with its head restrained using the PEEK pipes and stainless steel rods. Under anesthesia with ketamine hydrochloride (8 mg/kg body weight, i.m.) and xylazine hydrochloride (0.5 mg/kg, i.m.), the skull over the M1 and SMA contralateral to the hand for the task performance

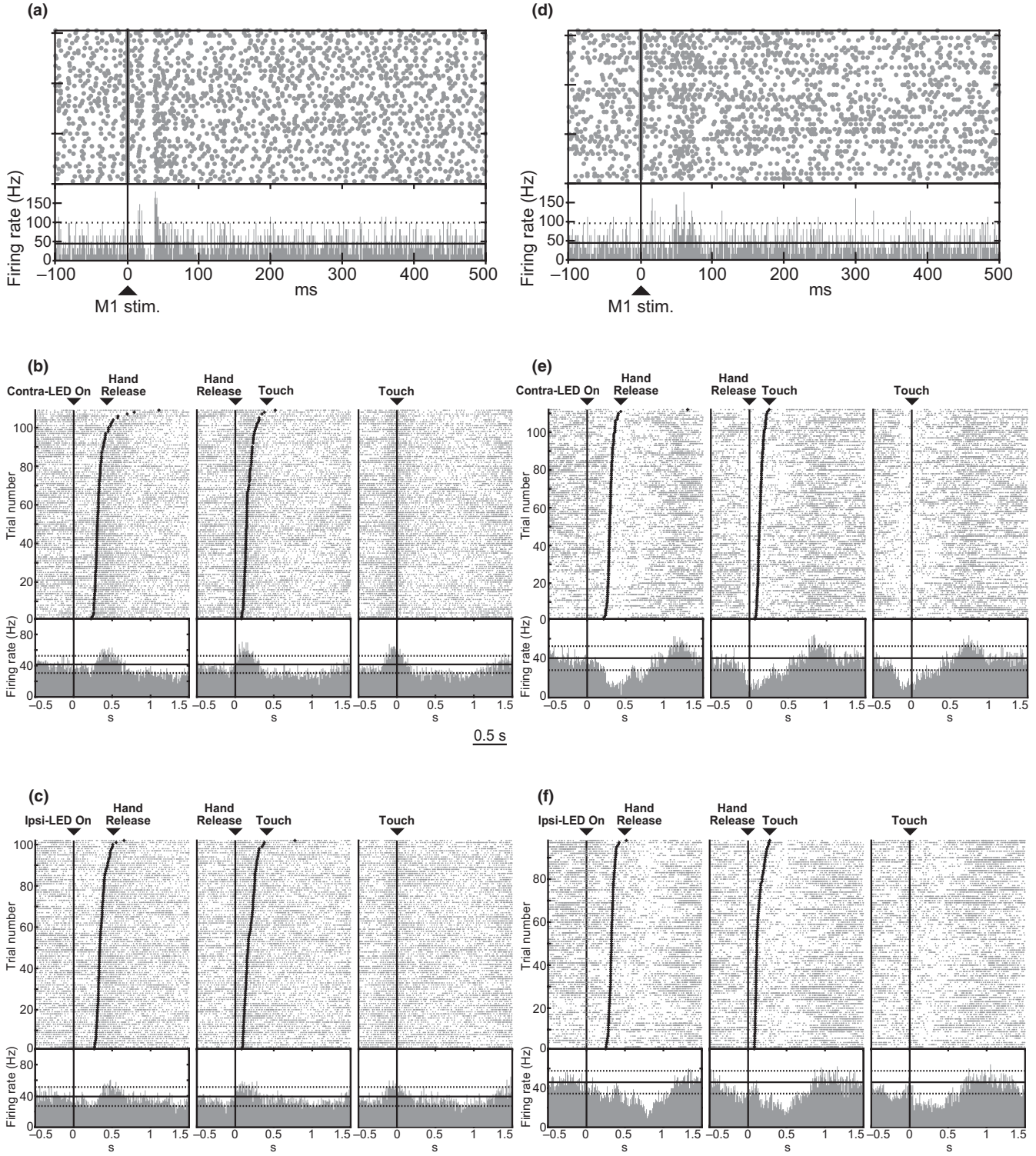

FIGURE 2 Example of activity of two GPe neurons (a, b, c; d, e, f) recorded in *Monkey H*. (a, d) Raster plots and peri-stimulus time histograms (PSTHs) in response to the electrical stimulation of the forelimb region of the M1. Cortical stimulation was delivered at time 0 (vertical lines and arrows). The black horizontal continuous and dotted lines in PSTHs represent the mean firing rate and the statistical level of $p < .05$, respectively. (b, c, e, f) Raster plots and peri-event time histograms (PETHs) of the same GPe neurons during the hand-reaching task in the Contra-LED (b, e) and Ipsi-LED (c, f) trials. Neuronal firings were aligned with the timing of each task event (LED On, Hand Release and Touch; represented by black vertical lines) in the order of reaction time (between LED On and Hand Release) or movement time (between Hand Release and Touch). The black horizontal continuous and dotted lines in PETHs represent the mean firing rate and the statistical level of $p < .05$, respectively. The GPe neuron in (b, c) increased its firing rate in both the Hand Release and Touch periods in both the Contra- and Ipsi-LED trials (thus, classified as "HR/$T_{\text{both LED}}$ with increasing activity" in Table 3), and the GPe neuron in (e, f) decreased its firing rate in both the Hand Release and Touch periods in the Contra-LED trials and in the Touch period in the Ipsi-LED trials (classified as HR/$T_{\text{one LED}}$/$T_{\text{the other LED}}$ with decreasing activity).

was removed. According to electrophysiological mapping, two pairs of bipolar stimulating electrodes (impedance, 30 kΩ at 1 kHz) made of 200-μm-diameter Teflon-coated stainless steel wires (inter-tip distance, 2 mm) were chronically implanted into the forelimb region of the M1, and one pair was implanted into the forelimb region of the SMA (Figure 1c) (for details, see Nambu et al., 2000, 2002a). Exposed areas were covered with transparent acrylic resin with the exception of the lateral M1 area (10–15 mm in diameter) for access to the GPe/GPi. A rectangular plastic chamber that covered the exposed brain area was fixed to the skull with acrylic resin.

2.5 | Multichannel recording of GPe/GPi activity

First, we roughly mapped the forelimb regions in the GPe/GPi receiving inputs from the forelimb regions of the M1/SMA 4–7 days after implantation of the stimulating electrodes. A glass-coated tungsten microelectrode (0.5 MΩ at 1 kHz, Alpha Omega) was inserted obliquely (40° from vertical in the frontal plane) into the GPe/GPi contralateral to the hand for the task performance using a hydraulic microdrive (MO-81-S; Narishige Scientific Instrument Lab). When penetrating the dura, lidocaine was applied as a local anesthetic. Signals from each channel were amplified, filtered at 0.3–5 kHz, converted to digital pulses using a home-made time-amplitude window discriminator and sampled at 2 kHz on a computer. The GPe and GPi were identified by their characteristic firing patterns: GPe neurons fire at high frequencies with pauses, whereas GPi neurons fire continuously at high frequencies without any pauses (DeLong, 1971). The GPe/GPi border was also identified by border neurons with middle-frequency regular firings and silent zones corresponding to the medial medullary lamina. The forelimb regions of the GPe/GPi were identified based on the responses to passive forelimb movements and responses to cortical stimulation. Electrical stimulation was applied to the forelimb regions of the M1/SMA (0.3-ms duration monophasic single pulse, 0.7-mA strength, at 0.7 Hz), and peri-stimulus time histograms (PSTHs, bin width of 1 ms, 100 trials) were constructed. GPe/GPi neurons with cortical inputs typically responded in a triphasic response pattern composed of early excitation, inhibition and late excitation (Nambu et al., 2000; Iwamuro et al., 2017).

Multichannel recording sessions were conducted once or twice per day, 3 days per week for several months. A multichannel recording electrode (Plextrode U-Probe; Plexon Inc.) consisting of 16 contacts (275 ± 50 kΩ at 1 kHz) in linear formation (inter-contact spacing, 150 μm) was used. The electrode was inserted obliquely (40° from vertical in the frontal plane) through a guide tube (outer diameter, 570 μm; inner diameter, 450 μm) into the forelimb regions of the GPe/GPi based on the mapping (Figure 1c) using a hydraulic microdrive (MO-971-S; Narishige Scientific Instrument Lab). When penetrating the dura, lidocaine was applied as a local anesthetic. Signals from each channel were amplified, filtered at 0.5–7 kHz, sampled at 25 kHz and stored using a multichannel recording system (RZ2 BioAmp Processor; Tucker-Davis Technologies). The following data were obtained from each neuron: (a) spontaneous activity; (b) activity in response to cortical stimulation (0.3-ms duration monophasic single pulse, 0.7-mA strength, at 0.5–0.7 Hz, at least 60 trials) through chronically implanted electrodes in the M1 and SMA; and (c) activity during performance of the hand-reaching task (at least 200 successful trials/session).

2.6 | Data analysis

Multichannel recording data were analyzed off-line to isolate spike events of individual neurons using OpenSorter software (Tucker-Davis Technologies). Autocorrelograms were constructed from the spike events to evaluate isolation quality. If any evidence of multiple cells or noise inclusion was found, the unit was re-isolated or excluded from further analyses. MATLAB software (R2018b; MathWorks) was used in the following analyses.

2.6.1 | Response to cortical stimulation

For the analysis of responses to cortical stimulation, PSTHs (bin width of 1 ms; pre-stimulation 100 ms, post-stimulation 500 ms) were constructed for at least 60 stimulation trials and then smoothed with a Gaussian kernel of $\sigma = 1.6$ ms. The mean and SD of the firing rate were calculated during the 100 ms preceding the onset of stimulation from the PSTH of each neuron, and were considered the baseline discharge rate. An increase in firing activity in response to stimulation was judged to be significant if firing rates during at least two consecutive bins (2 ms) exceeded the statistical level of the mean + 1.65 SD (corresponding to $p < .05$, one-tailed z test; Nambu et al., 2000; Iwamuro et al., 2017). A decrease in firing activity was similarly judged to be significant if firing rates during at least two consecutive bins (2 ms) dropped below the statistical level of the mean −1.65 SD. The latency of each response was defined as the time at which the first bin of the two consecutive bins exceeded this significance level. The responses were judged to end when two consecutive bins fell below this significance level.

2.6.2 | Firing rate changes during the task performance

GPe/GPi neurons that showed significant responses to M1 and/or SMA stimulation were used for the analysis of neuronal

activity during the performance of the hand-reaching task. GPe/GPi unit activity during the performance was aligned with the task events, such as LED On, Hand Release and Touch, and peri-event time histograms (PETHs, bin width of 10 ms) were constructed. The mean firing rate was calculated during the 100 ms preceding LED On, and the significance level ($p < .05$, two-tailed) was calculated assuming a z-distribution. If firing rates exceeded this confidence interval, the firing rate increase or decrease was considered significant. The time periods of Hand Release and Touch were defined as the 200-ms periods centered at Hand Release/Touch events.

2.6.3 | Correlated activity

To detect correlated activity in the specific timing, we segmented whole task periods into the following 100-ms periods: Before LED On, Before Hand Release and Before Touch periods were defined as the 100-ms periods before the corresponding events. After LED On, After Hand Release and After Touch periods were defined as the 100-ms periods after the corresponding events. Then, correlated activity of neuronal spiking was analyzed by using the following two-step methods.

In the first step, cross-correlations (bin width of 1 ms) were calculated from the 100-ms time periods and averaged across trials. The permuted cross-correlations under the null hypothesis of no correlated activity were obtained by rearranging the trial number of one neuron randomly and averaging across trials. After repeating the arrangement 1,000 times, 1,000 control correlation scores were obtained at each lag time and arranged from the smallest to the largest. The neuronal pair was defined as positively correlated if the original correlation score was higher than the 998th score among 1,000 permuted correlation scores; similarly, the pair was defined as negatively correlated if the original score was lower than the third score, roughly corresponding to a two-tailed test with $p < .005$. Statistical analysis was performed at each lag time from −3 to +3 ms.

To reduce false positives due to multiple comparisons, in the second step, a PETH (bin width of 2 ms) of correlated spiking events was constructed in the event period with a significant correlation. Spiking events of "neuron 1," when they preceded spikes of "neuron 2" by the lag time obtained in the first step, were used. Similar to the first step, the trial number of one neuron was randomly rearranged 1,000 times to calculate the permuted PETH and arranged from the smallest to the largest, and the significant deviation of the original PETH was examined during the same task period, that is, 100 ms before or after the task event timing. At each PETH bin, the original PETH was examined to identify the bin that was larger than the 995th among 1,000 permuted PETHs for the pairs with positive peaks in the cross-correlogram, and examined to identify the bin that was smaller than the 6th among 1,000 permuted PETHs for those with negative peaks, corresponding to a one-tailed test with $p \leq .005$. Only neuronal pairs that resulted in rejection of the null hypothesis in both the first and second steps were considered to have correlated activity during task performance. Based on the simulation study of the two-step statistical analysis using artificially generated spike trains (Methodological consideration and Figure S1), the minimum detectable correlation was from 0.0342 to 0.0444, and the false-positive rate was 0.47%. We examined six task periods, and the false-positive rate was estimated to be 2.8% in total, suggesting that these analyses have sufficient power to detect weak correlations and low false-positive rates.

The amplitude of significantly correlated activity was evaluated by calculating Pearson correlation coefficients. Given binary spike trains x_t, y_t (0 or 1, bin width of 1 ms) of a pair of neurons, x_t and $y_{t+\tau}$ with lag time τ of the significant correlation from −3 ms to +3 ms were scatter-plotted in the x-y plane. Then, a Pearson correlation coefficient was calculated. Correlation coefficients with non-significant peaks or troughs in the same task period were also calculated for comparison. The duration of significantly correlated activity was evaluated by the cross-correlogram in the first step.

A neuronal pair was considered to be correlated if it showed a significant peak in either Contra- or Ipsi-LED trials. To calculate the percentage of the number of neuronal pairs, the Before Hand Release and After Hand Release periods were combined as the Hand Release period, and the Before Touch and After Touch periods as the Touch period. Due to the high success rates (*Monkey H* ≥ 95%; *Monkey L* ≥ 84%), sufficient neuronal data could not be sampled for the analysis of error trials.

3 | RESULTS

3.1 | Neuronal activity evoked by cortical stimulation

The activity of two to five neurons was recorded from 16 contacts of the electrode. Among the well-isolated neurons, electrical stimulation of the forelimb regions of the M1 and/or SMA induced responses in a total of 140 GPe and 79 GPi neurons in *Monkeys H* and *L* combined (Table 1). Most of them (199/219, 91%; GPe, 123/140, 88%; GPi, 76/79, 96%) responded to both M1 and SMA stimulation. The response pattern was typically triphasic, that is, early excitation followed by inhibition and late excitation (Figure 2a), as reported previously (Nambu et al., 2000; Iwamuro et al., 2017). The latency and duration of these response components are shown in Table 2, and results agree with previous studies (Nambu et al., 2000; Iwamuro et al., 2017). The

TABLE 1 Number of GPe/GPi neurons that responded to cortical stimulation

	GPe			GPi			
Cortical stimulation	***Monkey H***	***Monkey L***	**Subtotal**	***Monkey H***	***Monkey L***	**Subtotal**	**Total**
M1	14	0	14 (10%)	2	1	3 (4%)	17 (8%)
M1 + SMA	83	40	123 (88%)	37	39	76 (96%)	199 (91%)
SMA	2	1	3 (2%)	0	0	0 (0%)	3 (1%)
Total	99	41	140	39	40	79	219

Numbers of neurons in the external (GPe) and internal (GPi) segments of the globus pallidus that responded to the stimulation of the forelimb regions of the primary motor cortex (M1) and the supplementary motor areas (SMA) in *Monkeys H* and *L*. M1, neurons responded only to M1 stimulation, M1 + SMA, neurons responded to both M1 and SMA stimulation, SMA, neurons responded only to SMA stimulation.

mean spontaneous firing rates of GPe neurons were 71 ± 29 (*Monkey H*) and 91 ± 28 (*Monkey L*) Hz, and those of GPi neurons were 75 ± 25 (*H*) and 100 ± 26 (*L*) Hz, which also agree with the previous studies. Both the GPe and GPi have clear somatotopic organization (Iwamuro et al., 2017), and these responsive GPe/GPi neurons were considered to be located in the forelimb regions of the GPe/GPi and were used for further analyses.

3.2 | Firing rate changes during the task performance

The neuronal activity of GPe and GPi neurons during the task performance was recorded, and PETHs were constructed to examine patterns of movement-related activity changes. Figure 2 shows typical examples of two GPe neurons recorded in *Monkey H*. A GPe neuron in Figure 2a–c responded to stimulation of the forelimb region of the M1 (Figure 2a) but not to SMA stimulation. This neuron increased its firing rate in both the Hand Release and Touch periods in both the Contra- and Ipsi-LED trials (Figure 2b,c). Another GPe neuron in Figure 2d–f that responded to stimulation of the forelimb regions of the M1 (Figure 2d) and SMA (data not shown) decreased its firing rate in both the Hand Release and Touch periods in the Contra-LED trials (Figure 2e) and in the Touch period in the Ipsi-LED trials (Figure 2f).

GPe/GPi neurons were classified by firing patterns during the task performance (Table 3). The majority of recorded GPe (115/140, 82%) and GPi (57/79, 72%) neurons in the forelimb regions exhibited firing rate changes during the Hand Release and/or Touch periods. The majority of them (79%; GPe, 93/115, 81%; GPi 43/57, 75%) exhibited changes in both Contra- and Ipsi-LED trials (GPe, $p < .0001$; GPi, $p = .0048$, chi-square test). Most neurons (GPe, 100/115, 87%; GPi, 47/57, 82%) showed simple response patterns, such as similar response patterns during both Contra- and Ipsi-LED trials (as shown in Figure 2b,c), and similar response patterns during both the Hand Release and Touch periods (as shown in Figure 2e,f), except that some neurons showed complex response patterns, such as a firing rate increase during the Hand Release period and a firing rate decrease during the Touch period, an increase in Contra-LED trials and a decrease in Ipsi-LED trials, or combinations of both. Among neurons showing similar response patterns, a large fraction showed a firing rate increase rather than a decrease (ratio of firing rate increase neurons vs. firing rate decrease neurons was 3.5 in the GPe

TABLE 2 Latency and duration of cortically evoked responses

	M1			SMA		
	Early excitation	**Inhibition**	**Late excitation**	**Early excitation**	**Inhibition**	**Late excitation**
GPe						
n	129	105	74	105	66	29
Latency	11.6 ± 4.0	23.7 ± 5.5	38.0 ± 7.6	12.8 ± 5.1	23.0 ± 7.5	37.4 ± 8.6
Duration	9.8 ± 5.2	16.4 ± 18.6	30.2 ± 18.5	6.8 ± 4.9	12.9 ± 20.8	14.0 ± 9.3
GPi						
n	67	49	17	56	33	9
Latency	11.1 ± 5.5	24.3 ± 8.6	38.9 ± 9.0	13.0 ± 3.8	22.2 ± 7.9	36.2 ± 15.1
Duration	10.7 ± 10.4	11.0 ± 5.9	19.7 ± 16.4	6.4 ± 3.9	11.3 ± 6.4	8.4 ± 3.9

Latencies and durations (mean ± SD in ms) of cortically evoked early excitation, inhibition and late excitation of GPe and GPi neurons in response to M1 and SMA stimulation. n, number of neurons showing early excitation, inhibition or late excitation among 140 GPe and 79 GPi neurons.

TABLE 3 Number of GPe/GPi neurons classified by firing patterns during task performance

Contra- or Ipsi-LED		Both LEDs		No modulation	Total
GPe					
$HR_{one\ LED}$	6 (3/3/0)	$HR_{both\ LEDs}$	6 (3/2/1)		12 (9%)
$T_{one\ LED}$	10 (8/2/0)	$T_{both\ LEDs}$	11 (7/3/1)		21 (15%)
$HR/T_{one\ LED}$	6 (6/0/0)	$HR/T_{both\ LEDs}$	42 (33/5/4)		82 (58%)
		$HR/T_{one\ LED}/HR_{the\ other\ LED}$	13 (7/2/4)		
		$HR/T_{one\ LED}/T_{the\ other\ LED}$	15 (10/2/3)		
		$HR_{one\ LED}/T_{the\ other\ LED}$	6 (1/3/2)		
				25	25 (18%)
Total	22 (17/5/0)		93 (61/17/15)	25	140 (78/22/15)
GPi					
$HR_{one\ LED}$	4 (2/2/0)	$HR_{both\ LEDs}$	5 (5/0/0)		9 (11%)
$T_{one\ LED}$	9 (6/3/0)	$T_{both\ LEDs}$	11 (10/1/0)		20 (25%)
$HR/T_{one\ LED}$	1 (1/0/0)	$HR/T_{both\ LEDs}$	13 (6/3/4)		28 (36%)
		$HR/T_{one\ LED}/HR_{the\ other\ LED}$	4 (2/0/2)		
		$HR/T_{one\ LED}/T_{the\ other\ LED}$	9 (6/0/3)		
		$HR_{one\ LED}/T_{the\ other\ LED}$	1 (0/0/1)		
				22	22 (28%)
Total	14 (9/5/0)		43 (29/4/10)	22	79 (38/9/10)

Numbers of GPe and GPi neurons showing significant firing rate changes during the Hand Release (HR) and/or Touch (T) periods in either Contra- or Ipsi-LED trials (Contra- or Ipsi-LED) or both Contra- and Ipsi-LED trials (both LEDs) in two monkeys. Numbers in parentheses showed number of neurons increasing their activity in the specific task event/ number of neurons decreasing their activity/ number of neurons showing complex response patterns. Complex response patterns include firing rate increases during the Hand Release period and firing rate decreases during the Touch period, increases in Contra-LED trial and decreases in Ipsi-LED trials, or combinations of both.

and 4.2 in the GPi, Table 3). Further detailed analyses of task-related firing properties were not performed because they are not the focus of the present study.

3.3 | Cross-correlated activity during task performance

Synchronized activity was examined in simultaneously recorded GPe/GPi neurons (184 GPe-GPe, 62 GPe-GPi and 71 GPi-GPi neuronal pairs) for possible correlations during each task period. Figure 3 shows a typical example of a GPe-GPe neuronal pair in *Monkey H* simultaneously recorded from channels 2 (GPe1) and 9 (GPe2), which were spaced 1.05 mm apart. GPe1 started to increase its activity after Touch, whereas GPe2 increased its activity preceding Touch in the Ipsi-LED trials (Figure 3a). Cross-correlograms of this neuronal pair were constructed for each period of the reaching task (the first step, Figure 3b). A significant but small and short (single bin, 1 ms) correlation was observed with a lag time of –3 ms during the Before Touch period (* at Before Touch in Figure 3b). The correlation of this neuronal pair was further examined by constructing PETHs of the correlated spike events with the lag time of –3 ms along the time course of the hand-reaching task (the second step, Figure 3c). The correlated spike events were increased above the chance level at 20 ms before Touch (* in Figure 3c, single bin, 2 ms, $p < .005$, permutation test; *See* Materials and Methods for details). In conclusion, this neuronal pair was considered to have significantly positive, but short correlated activity before Touch. This neuronal pair did not show any significant correlations during other task periods. In the Contra-LED trials, this neuronal pair, GPe1 and GPe2, similarly increased their firing rates in relation to Touch, but did not show any significant correlations in any task periods (data not shown). A significant correlation was observed in a specific task event in either Contra- or Ipsi-LED trials; thus, the correlation may have functional significance.

Among all neuronal pairs examined during each task event, such as the Before LED On, After LED On, Hand Release and Touch periods, only a small fraction (GPe-GPe, 2–8%; GPe-GPi, 0–13%; GPi-GPi, 1–6%) showed correlated activity (Figure 4), most of the correlated neuronal pairs showed a significant peak in a single task event of either Contra- or Ipsi-LED trials except for one GPe-GPe pair, suggesting that correlated activity was task selective and direction selective. A large fraction of the correlated neuronal pairs showed positive correlations: Positive-to-negative ratio was 6.0 in the

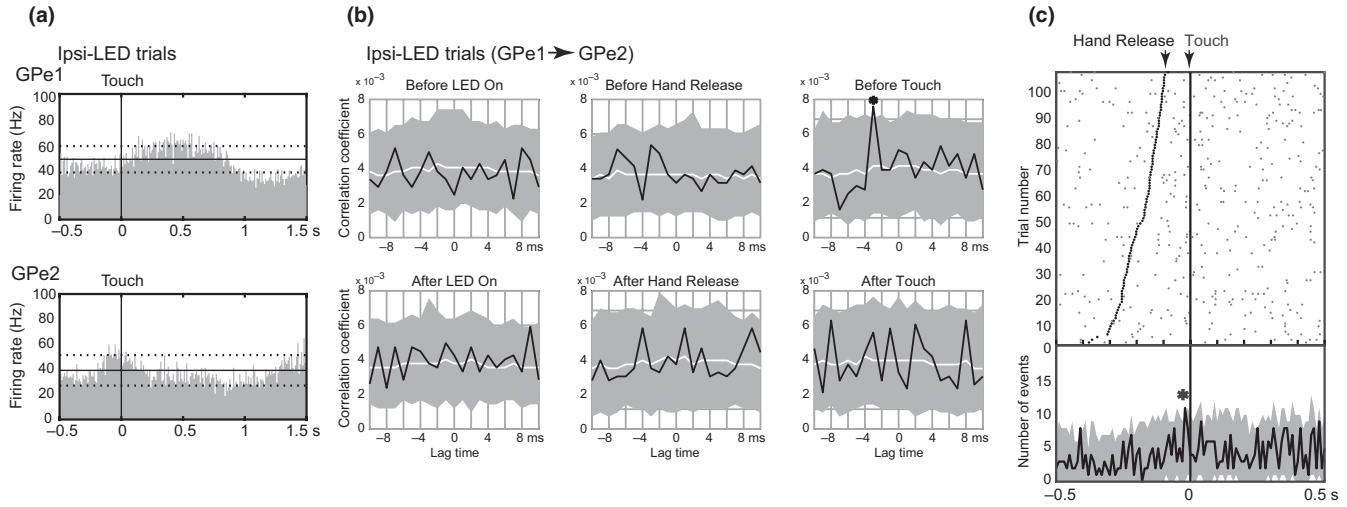

FIGURE 3 Example of cross-correlation analyses of a GPe-GPe pair (GPe1 and GPe2) simultaneously recorded in *Monkey H*. (a) PETHs of GPe1 and GPe2 neurons were aligned with the timing of Touch in the Ipsi-LED trials. (b) Cross-correlograms of the GPe-GPe pair were constructed during the Before LED On, After LED On, Before Hand Release, After Hand Release, Before Touch and After Touch periods. The black line, white line and shaded area in each graph represent the cross-correlogram, median and 99.5% confidence interval of permuted cross-correlograms, respectively. * represents a significant positive correlation (with a lag time of –3 ms, Before Touch). (c) Correlated spike events with a specific lag time along the time course of the hand-reaching task. Correlated neuronal spikes during the Touch period with a lag time of –3 ms were used for this analysis. The upper panel shows a raster plot of the correlated spike events. The black dots and vertical line in the upper panel represent the timing of Hand Release and Touch, respectively. The lower panel shows the PETH of the neuronal pair (black line) and the confidence interval (shaded area). * represents a significant positive correlation

GPe-GPe, 4.7 in the GPe-GPi and 1.8 in the GPi-GPi pairs. The proportions of neuronal pairs with positive, negative and no correlations were not significantly different among task events in the GPe-GPe, GPe-GPi or GPi-GPi pairs ($p > .05$, chi-square test; Figure 4). This means that the proportions of neuronal pairs with correlated activity were not increased during hand-reaching movements (Hand Release and/or Touch periods) from the resting periods (Before LED On and After LED On periods). Moreover, correlated neuronal pairs showed a significant peak in a single task event of either Contra- or Ipsi-LED trials, suggesting that correlated activity was task selective and direction selective. In total, 20% of neuronal pairs (GPe-GPe, 19%; GPe-GPi, 27%; GPi-GPi, 15%) showed correlated activity during one task event among the four.

Durations and amplitudes of the correlated activity were evaluated. Durations of all significant correlations were 1 ms. Amplitudes of significant and non-significant correlations (Pearson correlation coefficients) are plotted in Figure 5. Amplitudes of positive (gray circles), non-significant (white circles) and negative (black circles) correlations were continuously but separately distributed in GPe-GPe, GPe-GPi and GPi-GPi pairs. These observations indicate that durations and amplitudes of correlations were small and short, but significant.

Based on their activity changes during task events, GPe/GPi neuronal activity pairs were classified into groups with significant – significant [(+) - (+)], significant – non-significant [(+) - (–)] and non-significant – non-significant [(–) - (–)] firing rate changes in the Hand Release and Touch periods. The numbers of pairs with significantly correlated activity (Table 4) were evenly distributed among groups with and without firing rate changes in the corresponding task periods. This observation suggests that correlated activity may convey signals independently from firing rate changes.

Figure 6 shows the distribution of lag times for the correlated activity of GPe-GPe, GPe-GPi and GPi-GPi neuronal pairs during the Before LED On, After LED On, Hand Release and Touch periods. Lag times were evenly distributed in GPe-GPe and GPi-GPi pairs. On the other hand, in GPe-GPi pairs, GPe activity preceded GPi activity by 1 ms during the Hand Release period, and both neurons were simultaneously activated during the Touch period.

3.4 | Locations of recorded neuronal pairs

Figure 7 shows the locations of GPe/GPi neuronal pairs that exhibited correlated activity during the Before LED On, After LED On, Hand Release and Touch periods in *Monkey H*. As expected, they were located within the forelimb regions of the GPe and GPi (Iwamuro et al., 2017). The distance between correlated pairs varied extensively (*Monkey H*: GPe-GPe pairs, 680 ± 552 μm, $n = 30$; GPe-GPi pairs, 1419 ± 393 μm, $n = 13$; GPi-GPi pairs, 413 ± 195 μm, $n = 4$; *Monkey L:* GPe-GPe pairs, 720 ± 514 μm, $n = 5$; GPe-GPi

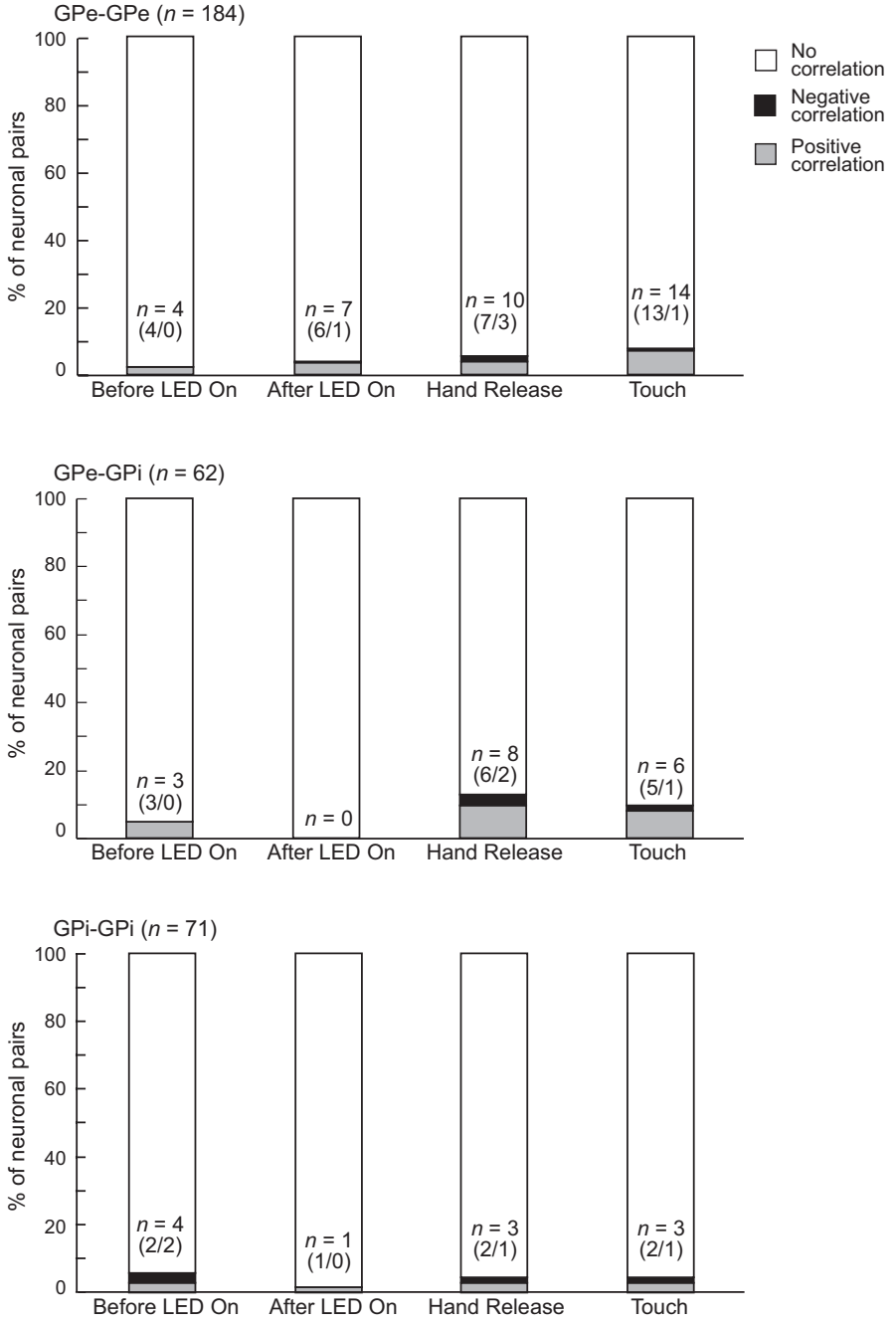

FIGURE 4 Proportions of GPe/GPi neuronal pairs with significantly correlated activity during the task performance. Proportions of GPe-GPe, GPe-GPi and GPi-GPi pairs with positive (gray), negative (black) and no (white) correlations are shown during the Before LED On, After LED On, Hand Release and Touch periods. *n* indicates the number of pairs with correlated activity in each period. Numbers in parentheses indicate number of pairs with positive correlations/ number of pairs with negative correlations

pairs, 1,275 ± 327 μm, $n = 4$; GPi-GPi pairs, 729 ± 305 μm, $n = 7$). The major distance was rather short (300 μm; 30%). Longer distances of up to 1,950 μm were also observed between GPe-GPi pairs.

4 | DISCUSSION

In this study, GPe/GPi neurons in monkeys showed firing rate changes during hand-reaching movements, which is in accordance with previous studies (DeLong, 1971; Hamada et al., 1990; Nambu et al., 1990; Mushiake & Strick, 1995; Turner & Anderson, 1997). Therefore, signals for motor control seem to be coded by firing rate changes in GPe/GPi neurons. On the other hand, GPe/GPi neurons may also utilize correlated activity to effectively convey information to their target nuclei. In the present study, we examined GPe/GPi neuronal cross-correlations in behaving monkeys and obtained the following results: (a) Most (79%) of the GPe/GPi neurons receiving inputs from the motor cortices exhibited task-related activity changes; and (b) a small number (20%) of GPe/GPi pairs showed correlated activity, and their number did not increase during movements, even though their firing rates were changed. Thus, firing rate coding, but not correlated activity coding, seems to play a primary role in information processing in the GPe/GPi.

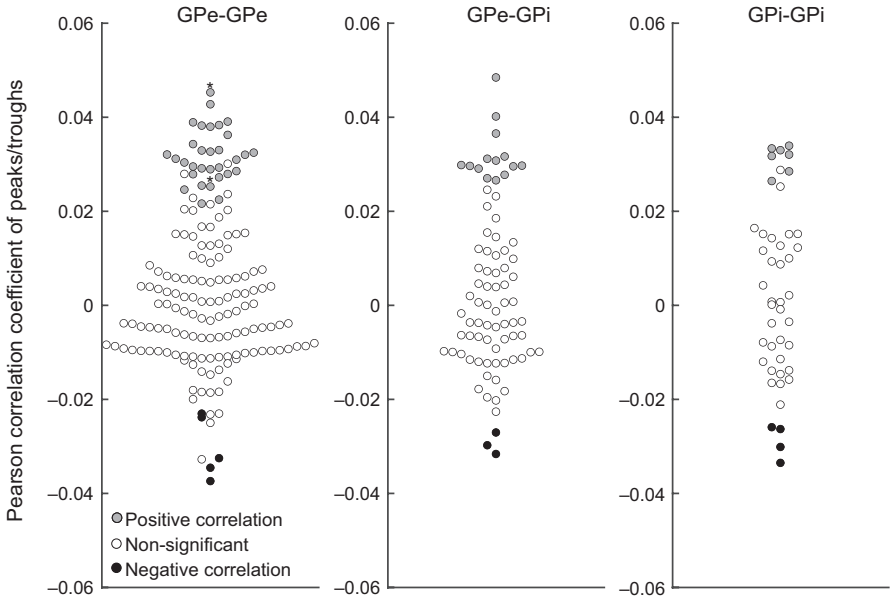

FIGURE 5 Distribution of Pearson correlation coefficients for significant and non-significant correlations (after two-step analysis). Gray and black circles represent amplitudes of significant peaks (i.e., positive correlation) and troughs (negative correlation), respectively. Non-significant peaks and troughs found in –3 to +3 ms lag times of the same cross-correlogram are shown as white circles. *, one GPe-GPe pair showed two significant positive peaks

TABLE 4 Number of pairs of GPe/GPi neurons with correlated activity classified by firing rate changes during the task performance

Firing rate changes	(+) - (+)	(+) - (–)	(–) - (–)
GPe-GPe			
Hand Release	2/100 (2%)	4/177 (2%)	4/91 (4%)
Touch	6/121 (5%)	6/181 (3%)	2/66 (3%)
GPe-GPi			
Hand Release	1/25 (4%)	4/67 (6%)	3/32 (9%)
Touch	3/45 (7%)	3/68 (4%)	0/11 (0%)
GPi-GPi			
Hand Release	1/29 (3%)	1/66 (2%)	1/47 (2%)
Touch	1/48 (2%)	1/60 (2%)	1/34 (3%)

GPe/GPi neuronal activity pairs were classified into groups with significant (+) and/or non-significant (–) firing rate changes during corresponding the Hand Release and Touch periods of the task. Among them, numbers and percentages of GPe/GPi neuronal activity pairs with significant correlations are indicated.

4.1 | Functional significance of correlated activity

Correlated activity among neuronal populations is observed in different brain regions, and may play a crucial role in information processing through neural networks (Singer, 1993; Salinas & Sejnowski, 2001; Rosenbaum et al., 2014). For example, frontal cortical neurons alter their correlated activity without significant changes in firing rates during motor task performance, especially between neighboring neurons (Vaadia et al., 1995). In the cerebellum, the synchronous inhibitory post-synaptic potentials of a small number of Purkinje cells generate time-locked action potentials to the cerebellar nuclear neurons through post-inhibitory rebound excitation, whereas asynchronous inputs simply suppress their firing (Person & Raman, 2011). Therefore, not only glutamatergic neurons in the cortex but also GABAergic neurons in the cerebellum seem to utilize correlated activity for signal transmission.

In contrast, in the present study, only a small fraction of GPe/GPi pairs showed correlated activity, and the peaks of the cross-correlograms were small and short. However, they showed correlated activity related to a specific task event, *for example*, a neuronal pair that exhibited correlated activity during the Before Touch period did not show correlated activity during the After Touch period (Figure 3). In addition, the appearance of correlated activity was specific to one movement direction except for one pair. Therefore, such correlated activity may play some functional roles.

The detection power and false-negative ratio of the two-step statistical analyses were evaluated, and they have sufficient detection power and a low false-negative rate (Methodological consideration and Figure S1). Other elements may affect the detection power. The chosen recording strategy using a linear array electrode does not rule out the possibility that correlations between the activity of neurons that are arranged clusters of different shapes would be missed by this study. Narrow lag times from –3 ms to +3 ms were used to reduce false-positive rates in the present study, but may prevent the detection of longer duration correlations as observed in Parkinson's disease (Nini et al., 1995; Raz et al., 2000). To examine this possibility, we constructed cross-correlograms at a longer range of –50 ms to +50 ms (Figure S2). However, we detected similar small and short correlated activity (Figure S2a) and evenly distributed lag times except

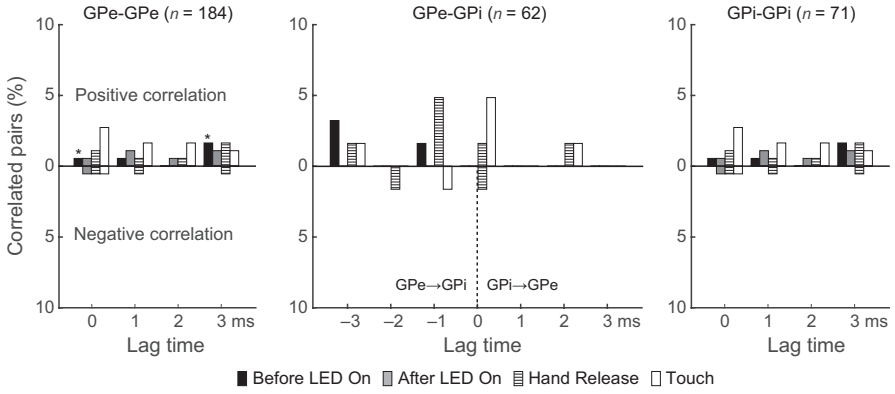

FIGURE 6 Distribution of lag times for correlated activity. Lag times of GPe-GPe, GPe-GPi and GPi-GPi neuronal pairs are represented during different task events, such as the Before LED On, After LED On, Hand Release and Touch periods, separately. *, one GPe-GPe pair showed two significant peaks in one and the other LED trials

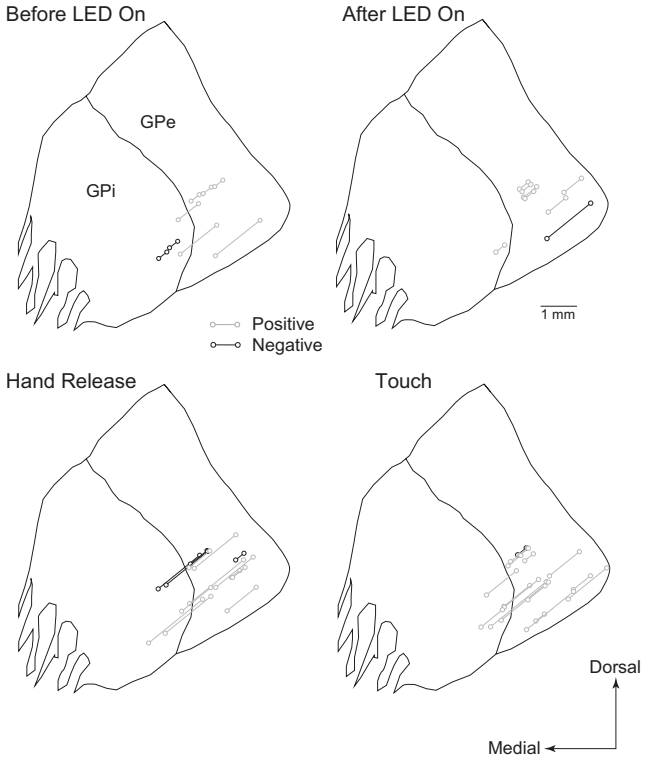

FIGURE 7 Locations of neuronal pairs with significant correlations in *Monkey H*. Neuronal pairs with positive and negative correlations are represented as gray and black connected circles, respectively, during the Before LED On, After LED On, Hand Release and Touch periods. Locations at three frontal planes (17, 16 and 15 mm anterior to the interaural line) are overlaid at the anterior 16-mm plane

for the peak at a lag time of 0 ms during the Touch period in GPe-GPi pairs (Figure S2b).

Some pairs showed a significant correlated activity in the Before LED on period (Figure 4). These are not related to task events and may reflect spontaneous correlated activity. Most of them were observed in either Contra- or Ipsi-LED trials, probably because weakly correlated activity fluctuated below the threshold and reached the threshold of either Contra- or Ipsi-LED trials by chance.

In addition to the spike-to-spike correlation examined in the present study, the spike count correlation that examines how similarly two neurons change their firing rates at a certain period of time and the signal correlation that examines how similarly two neurons respond to different signals are often assessed (Nevet et al., 2007; Cohen & Kohn, 2011). GPe/GPi neuronal activity pairs were classified based on their activity changes during task events into [(+) - (+)] (corresponding to significant signal correlation), [(+) - (–)] (no signal correlation) and [(–) - (–)] (no signal correlation). This observation in Table 4 suggests that the spike-to-spike correlation may convey signals independently from the signal correlation. The spike count correlation of GPe/GPi neuronal pairs remains to be studied (see Nevet et al., 2007).

4.2 | Mechanism of correlated activity

The GPe and GPi receive afferent inputs from the striatum and STN. The number of neurons in the striatum far exceeds that in the GPe/GPi, and thus, each GPe/GPi neuron receives convergent inputs from different striatal neurons (Flaherty & Graybiel, 1993; Parent & Hazrati, 1995; Levesque & Parent, 2005). On the other hand, the GPe/GPi receives divergent inputs from the STN (Hazrati & Parent, 1992; Parent & Hazrati, 1995; Sato et al., 2000). Correlated activity of GPe/GPi neurons may be based on the following mechanisms: (a) common inputs from the striatum and/or STN; and (b) inputs through local axon collaterals in the GPe or the GPe-GPi projections. Our results showed that only a small fraction (20%) exhibited correlated activity during the task performance, and most of them were positive cross-correlations (Figure 4). Positive rather than negative correlations suggest that inhibitory GPe local collaterals have little effect compared with common inputs from the striatum and/or STN, unless it is induced by disynaptic disinhibition. An anatomical study reported that an axon from a single striatal neuron formed several axon arbors in the GPe/GPi and that axon terminals from the STN covered larger areas of the GPe and GPi than striatal terminals (Parent & Hazrati, 1995). These anatomical

features may explain why neuronal pairs separated by a long distance (over 1 mm) showed correlated activity (Figure 7).

However, of note, such anatomical connections lead to the expectation of a much higher rate of correlated activity (Nevet et al., 2007), which was not the case in the present study. A small proportion of neuronal pairs with correlated activity during resting periods is consistent with previous reports (Nini et al., 1995; Raz et al., 2000; Bar-Gad et al., 2003). In addition, the present study provides the first evidence that correlated activity of GPe/GPi neurons does not significantly change during forelimb movements (Figure 4). These results suggest that the mechanism contributing to correlated activity in the GPe/GPi discussed above may be weak and that neighboring neurons deal with very different neuronal information (an extreme parallel computation) (Bar-Gad et al., 2003; Nevet et al., 2004, 2007). Other studies suggest an active decorrelating mechanism (Bar-Gad et al., 2003; Nevet et al., 2007; Wilson, 2013, 2015) based on their pacemaker-like activity. The majority of GPe/GPi neurons are functionally independent of each other and transfer motor signals to their target nuclei by firing rate changes.

4.3 | Clinical significance of correlated activity

Robust correlated oscillation was observed in the GPe/GPi of Parkinson's disease patients and animal models (Nini et al., 1995; Raz et al., 2000; Brown, 2007). These observations suggest that synchronized activity may disrupt appropriate information transmission to the thalamus. Taken together with our present results, weak or no correlations among GPe/GPi neurons may be necessary for the normal function of the basal ganglia and motor control. In addition, dopamine may reduce neuronal correlations to maintain parallel information processing in the basal ganglia.

In summary, the results of this study indicate that individual GPe/GPi neurons are activated independently rather than in concert, which may be necessary for normal information processing within the basal ganglia (Bar-Gad et al., 2003; Wilson, 2013, 2015). The alteration of this functional independency, increased neuronal synchronization, may induce motor control abnormalities such as those observed in Parkinson's disease (Nini et al., 1995; Bergman et al., 1998; Raz et al., 2000). Further studies are necessary to investigate the neuronal mechanisms of correlated activity within the GPe/GPi using animal models of movement disorders, which could lead to the development of more effective treatments.

ACKNOWLEDGEMENTS

We thank S. Sato, H. Isogai, N. Suzuki, K. Awamura, K. Miyamoto and Y. Sugiyama for their technical support and Y. Yamagata for her critical reading of the manuscript. This work was supported by MEXT KAKENHI ("Non-linear Neuro-oscillology," 15H05873 to AN), JSPS KAKENHI (18K15340 to TH, 16K07014 to SC, and 19KK0193 and 26250009 to AN), JST CREST (JPMJCR1853 to SC) and AMED (JP19dm0307005 to AN). The Japanese monkeys used in this study were provided through the National Bio-Resource Project (NBRP) "Japanese Monkeys" of AMED.

CONFLICT OF INTEREST

The authors declare no competing financial interests.

AUTHOR CONTRIBUTIONS

SC and AN designed the experiments; WW and SC performed the experiments; WW, TH and SC analyzed the data; and WW, TH, SC and AN wrote the manuscript.

PEER REVIEW

The peer review history for this article is available at https://publons.com/publon/10.1111/ejn.14903.

DATA AVAILABILITY STATEMENT

The data presented in this manuscript are available upon request to the corresponding author (nambu@nips.ac.jp).

ORCID

Woranan Wongmassang https://orcid.org/0000-0003-3870-8867
Satomi Chiken https://orcid.org/0000-0002-2679-9530
Atsushi Nambu https://orcid.org/0000-0003-2153-5445

REFERENCES

Alexander, G. E., & Crutcher, M. D. (1990). Functional architecture of basal ganglia circuits: neural substrates of parallel processing. *Trends in Neurosciences*, *13*, 266–271.

Alonso, J.-M., Usrey, W. M., & Reid, R. C. (1996). Precisely correlated firing in cells of the lateral geniculate nucleus. *Nature*, *383*, 815–819.

Bar-Gad, I., Heimer, G., Ritov, Y., & Bergman, H. (2003). Functional correlations between neighboring neurons in the primate globus pallidus are weak or nonexistent. *Journal of Neuroscience*, *23*, 4012–4016.

Bergman, H., Feingold, A., Nini, A., Raz, A., Slovin, H., Abeles, M., & Vaadia, E. (1998). Physiological aspects of information processing in the basal ganglia of normal and parkinsonian primates. *Trends Neuroscience*, *21*, 32–38.

Brown, P. (2007). Abnormal oscillatory synchronisation in the motor system leads to impaired movement. *Current Opinion in Neurobiology Motor Systems/Neurobiology of Behaviour*, *17*, 656–664.

Bruno, R. M. (2006). Cortex is driven by weak but synchronously active thalamocortical synapses. *Science*, *312*, 1622–1627.

Cohen, M. R., & Kohn, A. (2011). Measuring and interpreting neuronal correlations. *Nature Neuroscience*, *14*, 811–819.

de la Rocha, J., Doiron, B., Shea-Brown, E., Josić, K., & Reyes, A. (2007). Correlation between neural spike trains increases with firing rate. *Nature*, *448*, 802–806.

DeLong, M. R. (1971). Activity of pallidal neurons during movement. *Journal of Neurophysiology*, *34*, 414–427.

Flaherty, A. W., & Graybiel, A. M. (1993). Output architecture of the primate putamen. *Journal of Neuroscience*, *13*, 3222–3237.

Glajch, K. E., Kelver, D. A., Hegeman, D. J., Cui, Q., Xenias, H. S., Augustine, E. C., Hernandez, V. M., Verma, N., Huang, T. Y., Luo, M., Justice, N. J., & Chan, C. S. (2016). Npas1+ pallidal neurons target striatal projection neurons. *Journal of Neuroscience*, *36*, 5472–5488.

Hamada, I., DeLong, M. R., & Mano, N. (1990). Activity of identified wrist-related pallidal neurons during step and ramp wrist movements in the monkey. *Journal of Neurophysiology*, *64*, 1892–1906.

Hauber, W. (1998). Involvement of basal ganglia transmitter systems in movement initiation. *Progress in Neurobiology*, *56*, 507–540.

Hazrati, L.-N., & Parent, A. (1992). Convergence of subthalamic and striatal efferents at pallidal level in primates: An anterograde double-labeling study with biocytin and PHA-L. *Brain Research*, *569*, 336–340.

Hegeman, D. J., Hong, E. S., Hernández, V. M., & Chan, C. S. (2016). The external globus pallidus: Progress and perspectives. *European Journal of Neuroscience*, *43*, 1239–1265.

Iwamuro, H., Tachibana, Y., Ugawa, Y., Saito, N., & Nambu, A. (2017). Information processing from the motor cortices to the subthalamic nucleus and globus pallidus and their somatotopic organizations revealed electrophysiologically in monkeys. *European Journal of Neuroscience*, *46*, 2684–2701.

Kohn, A. (2005). Stimulus dependence of neuronal correlation in primary visual cortex of the macaque. *Journal of Neuroscience*, *25*, 3661–3673.

Levesque, M., & Parent, A. (2005). The striatofugal fiber system in primates: A reevaluation of its organization based on single-axon tracing studies. *Proceedings National Academy Sciences of United States of America*, *102*, 11888–11893.

Mushiake, H., & Strick, P. L. (1995). Pallidal neuron activity during sequential arm movements. *Journal of Neurophysiology*, *74*, 2754–2758.

Nambu, A., Yoshida, S., & Jinnai, K. (1990). Discharge patterns of pallidal neurons with input from various cortical areas during movement in the monkey. *Brain Research*, *519*, 183–191.

Nambu, A., Tokuno, H., Hamada, I., Kita, H., Imanishi, M., Akazawa, T., Ikeuchi, Y., & Hasegawa, N. (2000). Excitatory cortical inputs to pallidal neurons via the subthalamic nucleus in the monkey. *Journal of Neurophysiology*, *84*, 289–300.

Nambu, A., Kaneda, K., Tokuno, H., & Takada, M. (2002a). Organization of corticostriatal motor inputs in monkey putamen. *Journal of Neurophysiology*, *88*, 1830–1842.

Nambu, A., Tokuno, H., & Takada, M. (2002b). Functional significance of the cortico–subthalamo–pallidal 'hyperdirect' pathway. *Neuroscience Research*, *43*, 111–117.

Nevet, A., Morris, G., Saban, G., Fainstein, N., & Bergman, H. (2004). Discharge rate of substantia nigra pars reticulata neurons is reduced in non-parkinsonian monkeys with apomorphine-induced orofacial dyskinesia. *Journal of Neurophysiology*, *92*, 1973–1981.

Nevet, A., Morris, G., Saban, G., Arkadir, D., & Bergman, H. (2007). Lack of spike-count and spike-time correlations in the substantia nigra reticulata despite overlap of neural responses. *Journal of Neurophysiology*, *98*, 2232–2243.

Nini, A., Feingold, A., Slovin, H., & Bergman, H. (1995). Neurons in the globus pallidus do not show correlated activity in the normal monkey, but phase-locked oscillations appear in the MPTP model of parkinsonism. *Journal of Neurophysiology*, *74*, 1800–1805.

Parent, A., & Hazrati, L.-N. (1995). Functional anatomy of the basal ganglia. I. The cortico-basal ganglia-thalamo-cortical loop. *Brain Research Reviews*, *20*, 91–127.

Person, A. L., & Raman, I. M. (2011). Purkinje neuron synchrony elicits time-locked spiking in the cerebellar nuclei. *Nature*, *481*, 502–505.

Raz, A., Vaadia, E., & Bergman, H. (2000). Firing patterns and correlations of spontaneous discharge of pallidal neurons in the normal and the tremulous 1-methyl-4-phenyl-1,2,3,6-tetrahydropyridine vervet model of parkinsonism. *The Journal of Neuroscience*, *20*, 8559–8571.

Rosenbaum, R., Tchumatchenko, T., & Moreno-Bote, R. (2014). Correlated neuronal activity and its relationship to coding, dynamics and network architecture. *Frontiers in Computational Neuroscience*, *8*, https://doi.org/10.3389/fncom.2014.00102

Salinas, E., & Sejnowski, T. J. (2001). Correlated neuronal activity and the flow of neural information. *Nature Review Neuroscience*, *2*, 539.

Sato, F., Parent, M., Levesque, M., & Parent, A. (2000). Axonal branching pattern of neurons of the subthalamic nucleus in primates. *The Journal of Comparative Neurology*, *424*, 142–152.

Singer, W. (1993). Synchronization of cortical activity and its putative role in information processing and learning. *Annual Review of Physiology*, *55*, 349–374.

Turner, R. S., & Anderson, M. E. (1997). Pallidal discharge related to the kinematics of reaching movements in two dimensions. *Journal of Neurophysiology*, *77*, 1051–1074.

Vaadia, E., Haalman, I., Abeles, M., Bergman, H., Prut, Y., Slovin, H., & Aertsen, A. (1995). Dynamics of neuronal interactions in monkey cortex in relation to behavioural events. *Nature*, *373*, 515.

Wichmann, T., & DeLong, M. R. (1996). Functional and pathophysiological models of the basal ganglia. *Current Opinion in Neurobiology*, *6*, 751–758.

Wilson, C. J. (2013). Active decorrelation in the basal ganglia. *Neuroscience*, *250*, 467–482.

Wilson, C. J. (2015). Oscillators and oscillations in the basal ganglia. *The Neuroscientist*, *21*, 530–539.

SUPPORTING INFORMATION

Additional supporting information may be found online in the Supporting Information section.

How to cite this article: Wongmassang W, Hasegawa T, Chiken S, Nambu A. Weakly correlated activity of pallidal neurons in behaving monkeys. *Eur J Neurosci*. 2021;53:2178–2191. https://doi.org/10.1111/ejn.14903